Composite Structures 269 (2021) 114034

Contents lists available at ScienceDirect

Composite Structures

journal homepage: www.elsevier.com/locate/compstruct

Bond durability and service life prediction of BFRP bars to steel FRC under aggressive environmental conditions

Alaa Taha, Wael Alnahhal *

Department of Civil and Architectural Engineering, Qatar University, Doha, Qatar

ARTICLE INFO

Keywords:
Steel fiber-reinforced concrete
Bond durability
Durability
Basalt FRP bars
Bond test

ABSTRACT

This study presents an experimental investigation on the bond durability of helically wrapped basalt fiber reinforced polymer (BFRP) bars embedded in plain and steel fiber reinforced concrete (SFRC) under the combined effect of simulated oceanic environment and elevated temperatures. A total of sixty-three pullout specimens were tested to study the effect of concrete type (plain and SFRC), immersion temperature (35 °C and 60 °C), immersion duration (30, 60, and 90 days), and fiber volume fraction (V_f) of steel fibers (0.5% and 1%). The bond durability of the used bars was examined based on the bond strength and mode of failure. The BFRP bars at the interface along the embedment length with concrete were analyzed using scanning electron microscopy. In addition, the BPE and CMR models for bond-slip behavior were calibrated considering the immersion temperature, concrete type, and exposure duration. The experimental results revealed that the pullout specimens with V_f = 1% showed higher bond durability performance than specimens with V_f = 0.5%, particularly at high temperatures. Furthermore, the CMR model showed better correlation with the experimental data than the BPE model. Moreover, the 50 years service life prediction showed bond strength retentions of BFRP bars that ranged from 54% to 86% depending on the type of concrete (plain and SFRC), surrounding mean annual temperature (5 °C to 35 °C), and degree of moisture (dry, moist, and moisture saturated).

1. Introduction

Fiber reinforced polymers (FRP) bars are promising to be an effective solution that prevents the fast deterioration of infrastructures due to the corrosion of the conventionally used steel reinforcements [1]. As a result, many types of FRPs, such as glass (GFRP), carbon (CFRP), and aramid (AFRP), have been widely accepted and used as a strengthening and reinforcing material for reinforced concrete (RC) members. Recently, basalt FRP (BFRP) bars have emerged as a promising alternative to the commonly used GFRP bars [2–4]. However, current FRP design standards and specifications do not incorporate BFRP bars due to the limited studies on the durability performance of BFRP bars [5].

In general, the production process of basalt fibers is much safer for the environment than that of the glass fibers [6]. Therefore, for a wider acceptance of BFRP bars in the construction industry, further studies concerning several aspects such as their safety, sustainability, and structural behavior are required. One crucial aspect is the bond behavior of FRP bars with structural concrete. The bond behavior of FRP bars significantly influences the capacity, ultimate states, and serviceability of FRP-RC members. Additionally, previous studies have shown that the bond durability of FRP bars plays a significant role in affecting the durability of FRP-RC structures [7,8].

Several studies have been performed on the bond performance of FRP bars [9–14]. However, limited studies have investigated the effect of structural fibers on the bond performance of FRP bars and the bond durability of BFRP bars with concrete. Ding et al. [15] reported that adding a combination of steel fibers (SF) and macro-polypropylene fibers (PPA) into concrete improved the bond performance of GFRP bars to a level equivalent or even better than the bond performance of steel rebars embedded in plain concrete. Bi and Wang [16] observed a noticeable enhancement in BFRP bars' bond strength when 0.2% volume content of basalt fibers was added to the concrete mixture. Similarly, Solyom and Balazs [17] demonstrated that the addition of short fibers (SF, synthetic micro-fiber, and synthetic macro-fibers) to the concrete mix enhanced the bond behavior of different types of FRP bars (CFRP, GFRP, and BFRP bars). In contrast, Belarbi and Wang [18] reported that the addition of fibers had a negligible contribution on improving the bond strength of GFRP and CFRP bars in fiber reinforced concrete (FRC) and a moderate enhancement on the ductility response of the bars.

* Corresponding author.
E-mail addresses: at1301775@qu.edu.qa (A. Taha), wael.alnahhal@qu.edu.qa (W. Alnahhal).

https://doi.org/10.1016/j.compstruct.2021.114034
Received 22 April 2021; Accepted 28 April 2021
Available online 4 May 2021

In terms of bond durability of FRP bars, Hassan et al. [5] observed a reduction of 19% in the bond strength of BFRP bars when subjected to an alkaline environment at a temperature of 40 °C for six months compared to the unconditioned specimens. El Refai et al.[19] demonstrated that moisture environments had the most detrimental effect on the bond capacity of BFRP bars. Dong et al. [20] studied the bond durability of FRP bars in seawater for durations up to 60 days at different conditioning temperatures. The test results of their study showed bond strength reductions of 9.1% and 7.1% after 60 days at 40 °C for basalt-vinyl ester and glass-vinyl ester FRP bars, respectively, whereas the bond strength of basalt epoxy FRP bars remained unchanged. Moreover, Dong et al. [21] reported that direct immersion in seawater had a more severe effect on the bond strength of BFRP bars than wet-dry cycles with a reduction of 22% compared to the control specimens.

On the other hand, a limited number of studies investigated the effect of structural fibers on the bond durability of FRP bars to concrete [22–24]. Yan and Lin [22] investigated the effect of using steel and polyvinyl alcohol fibers on the bond degradation of sand-coated GFRP bars in a saline environment. The test results indicated an improvement in the bond strength of unconditioned and conditioned specimens with the addition of structural fibers regardless of their type. Out of the structural fibers used, SFRC at 1% volume fraction showed the highest enhancement on the bond strength of the used GFRP bars. On the contrary, Belarabi and Wang [23] studied the bond degradation of GFRP bars embedded in plain and polypropylene FRC. The environmental conditioning used in their study was cycles of free-thaw combined with high temperature cycles for 100 days. The test results showed that 8 mm GFRP bars embedded in FRC specimens resulted in lower bond strength values for unconditioned and conditioned specimens when compared to plain concrete specimens. Moreover, Taha et al. [24] studied the effect of basalt FRC on the bond durability of BFRP bars in seawater conditions. The study indicated that the addition of basalt fibers enhanced the bond durability of helically wrapped BFRP bars to concrete when subjected to extreme seawater conditions.

Based on the previous discussion, the studies on the bond durability of BFRP bars are limited and contradictory to a certain limit; therefore, further investigations are required on the bond degradation of BFRP bars with concrete under the combined effect of elevated temperatures and seawater conditions to enrich the literature. Moreover, only few studies have been conducted on the effect of FRC on the bond durability of FRP bars and were mainly conducted on the conventional GFRP bars. This study is part of an extensive research project conducted at Qatar University to assess experimentally and analytically the bond durability of BFRP bars. In the current study, the bond durability and service life prediction of BFRP Bars to the commonly available steel FRC under aggressive environmental conditions were evaluated.

2. Experimental program

2.1. Materials

2.1.1. Fiber reinforced concrete

The steel fibers used in this study are hook-ended steel fibers, as illustrated in Fig. 1(a). As provided by the manufacturer datasheet, the used steel fibers had a length of 50 mm, a diameter of 0.9 mm, an aspect ratio of 55, a tensile strength of 1100 MPa, and a density of 7.85 g/cm^3. The concrete mix ingredients are shown in Table 1. Two V_f of 0.5 and 1% were used in the FRC mix design. Trial mixes were performed to achieve the proper mix design with satisfactory concrete workability and fiber distribution. All specimens were prepared in the same conditions, including the control specimens.

2.1.2. Reinforcing bars

Helical wrapped BFRP bars were used in this study, as depicted in Fig. 1(b). The bars used consisted of indentations distanced at 3 cm. The BFRP bars tensile strength is 1100 MPa with an elastic modulus of 44 GPa, as reported in a previous study by the authors [24]. The density of the BFRP bars is 1.9 g/cm^3, which is almost four times less than that of conventional steel. All BFRP bars investigated in this study had a nominal diameter of 10 mm. The polymeric resin of the used bars is vinylester. The fibers of the bars investigated in this study are extracted from basalt rocks with the primary composition being silica oxide, composing up to 57.5% of the basalt fibers, which is greater than the minimum content of 46% recommended by Gutnikov et al. [25].

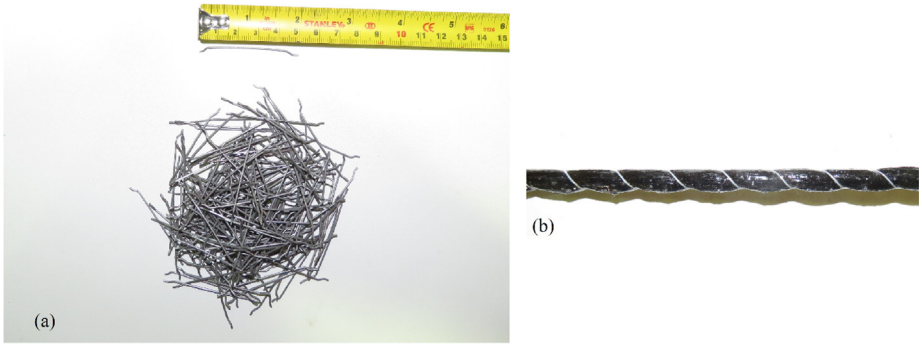

Fig. 1. Materials Used: (a) Steel Fibers; (b) BFRP Bar.

Table 1
Mix Design.

Mix Type	Fiber Type	Cement (kg/m^3)	Water (kg/m^3)	Sand (kg/m^3)	Coarse Aggregate (kg/m^3)	Fiber Volume Fraction (%)	Super-plasticizer (kg/m^3)
PC	Plain concrete	350	204	714	1082	0	0
Steel-0.5%	Hook ended steel	350	204	714	1082	0.5	0.27
Steel-1%	Hook ended Steel	350	204	714	1082	1	0.35

Table 2
Pullout Test Results.

Specimen	f'c (MPa)	τ_{max} (Mpa)	τ^*_{max} (MPa)	τ^*n (MPa)	δ_{LE} (mm)	δ_{FE} (mm)	τ_{ons} (MPa)	τ_r (MPa)	Failure Mode	Retention (%)
Unconditioned (Control) Specimens										
PC-C-1	32.5	13.14	13.14	2.3	7.18	8.65	0.39	12.51	PO	100
PC-C-2		11.78			6.2	6.21	1.49	9.58	PO	
PC-C-3		14.49			4.81	6.44	2.58	12.47	PO	
0.5%SF-C-1	33.1	15.97	15.7	2.73	7.31	9.22	0.11	14.23	PO	100
0.5%SF-C-2		16.58			5.14	N. A	0.04	13.55	PO	
0.5%SF-C-3		14.55			4.59	6.47	0.12	10.22	PO	
1%SF-C-1	31.1	13.11	13.34	2.39	6.24	7.19	0.22	11.93	PO	100
1%SF-C-2		14.34			6.23	6.76	0.16	12.44	PO	
1%SF-C-3		12.56			6.23	6.66	0.31	10.17	PO	
30 Days Conditioned Specimens at 35 °C										
PC-30–35-1	30.4	11.4	9.547	1.73	4.08	5.18	0.23	9.98	PO	73
PC-30–35-2		8.96			4.63	4.72	0.35	6.51	PO	
PC-30–35-3		8.28			7.82	8.61	0.29	7	PO	
0.5%SF-30–35-1	33.3	12.25	10.97	1.9	5.53	5.97	0.54	10.83	PO	70
0.5%SF-30–35-2		11.72			4.78	5.29	0.34	8.69	PO	
0.5%SF-30–35-3		8.93			4.98	5.54	0.29	5.52	PO	
1%SF-30–35-1	30.3	11.2	12.49	2.27	7.37	7.82	0.37	10.18	PO	94
1%SF-30–35-2		NA			N. A	N. A	N. A	N. A	N.A	
1%SF-30–35-3		13.77			6.11	6.01	0.49	12.12	PO	
30 Days Conditioned Specimens at 60 °C										
PC-30–60-1	29.3	12.14	13.4	2.48	6.26	6.59	0.12	10.45	PO	102
PC-30–60-2		13.38			6.54	7.01	0.42	10.46	PO	
PC-30–60-3		14.69			4.24	5.51	0.48	10.93	PO	
0.5%SF-30–60-1	31.1	11.81	10.54	1.89	4.19	4.83	0.51	9.52	PO	67
0.5%SF-30–60-2		8.01			5.51	5.13	0.54	6.45	PO	
0.5%SF-30–60-3		11.81			6.03	5.75	0.13	9.11	PO	
1%SF-30–60-1	35.5	13.48	14.15	2.37	4.8	5.82	0.17	10.63	PO	106
1%SF-30–60-2		14.92			5.92	6.36	0.19	12.4	PO	
1%SF-30–60-3		14.05			5.55	6.75	0.46	11.12	PO	
60 Days Conditioned Specimens at 35 °C										
PC-60–35-1	34.2	12.14	10.9	1.86	7.35	7.01	0.64	11.11	PO	83
PC-60–35-2		10.26			4.8	5.59	0.56	8.46	PO	
PC-60–35-3		10.31			3.64	4.09	0.51	6.63	PO	
0.5%SF-60–35-1	34.5	14.04	12.21	2.08	5.6	6.18	0.46	11.22	PO	78
0.5%SF-60–35-2		10.93			7.52	8.54	0.51	8.65	PO	
0.5%SF-60–35-3		11.66			8.03	8.36	0.63	10.77	PO	
1%SF-60–35-1	30.4	11.33	10.69	1.94	6.3	6.41	0.39	10.48	PO	80
1%SF-60–35-2		10.93			6.82	7.44	0.54	8.39	PO	
1%SF-60–35-3		9.81			7.86	8.16	0.28	8.97	PO	
60 Days Conditioned Specimens at 60 °C										
PC-60–60-1	34.4	16.34	12.17	2.07	3.9	3.97	0.09	11.74	PO /R	93
PC-60–60-2		11.65			6.81	7.07	0.11	10.44	PO	
PC-60–60-3		8.52			5	5.49	0.22	7.51	PO	
0.5%SF-60–60-1	31.8	11.95	10.12	1.79	6.01	5.93	0.35	8.78	PO	64
0.5%SF-60–60-2		9.56			6.08	6.02	0.62	6.98	PO	
0.5%SF-60–60-3		8.85			5.33	5.54	0.36	7.29	PO	
1%SF-60–60-1	37.1	14.41	13.72	2.25	4.53	6.03	0.29	10.71	PO	103
1%SF-60–60-2		NA			NA	NA	NA	NA	NA	
1%SF-60–60-3		13.02			3.28	4.25	0.25	11.75	PO	
90 Days Conditioned Specimens at 35 °C										
PC-90–35-1	35	14.22	12.14	2.05	4.52	5.2	0.3	11.14	PO	92
PC-90–35-2		9.96			5.7	5.85	0.15	8.3	PO	
PC-90–35-3		12.25			5.25	5.28	0.28	9.18	PO	
0.5%SF-90–35-1	34	10.37	9.157	1.57	4.4	4.48	0.89	8.57	PO	58
0.5%SF-90–35-2		9.95			4.93	5.54	0.28	8.84	PO	
0.5%SF-90–35-3		7.15			10.92	10.75	1.01	6.52	PO	
1%SF-90–35-1	31.2	10.32	10.53	1.89	4.49	4.87	0.41	8.49	PO	79
1%SF-90–35-2		11.95			4.44	4.62	0.21	8.09	PO	
1%SF-90–35-3		9.33			3.86	5.02	0.03	8.12	PO	
90 Days Conditioned Specimens at 60 °C										
PC-90–60-1	35.6	11.6	11.77	1.97	8.35	8.68	0.76	10.34	PO/R	90
PC-90–60-2		10.56			4.43	5.2	0.39	7.29	PO	
PC-90–60-3		13.15			5.57	4.824	1.74	NA	R	
0.5%SF-90–60-1	33.6	9.48	10.37	1.79	5.69	7.23	0.14	7.69	PO	66
0.5%SF-90–60-2		10.15			5.5	6.14	0.23	8.4	PO	
0.5%SF-90–60-3		11.48			4.94	7.15	0.04	8.44	PO	
1%SF-90–60-1	38	14.05	13.76	2.23	4.04	NA	0.05	11.79	PO	103
1%SF-90–60-2		13.14			3.58	4.29	0.24	8.38	PO	
1%SF-90–60-3		14.1			6.59	7.07[a]	1.19	13.17	PO	

Note: f'c: Concrete Compressive Strength; τmax: Bond Strength; τ*max: Average Bond Strength; $\tau^*n = \tau^*max/\sqrt{(fc')}$; δ_{LE} = Loaded End Slippage; δ_{FE}: Free End Slippage; τ_{ons}: Adhesion Stress τ_r: Residual Bond Strength; PO: Pullout Failure; R: Rebar Fracture; PO/R: Pullout Followed by Rebar Fracture; NA: data test not available .

2.2. Test specimens

Sixty-three pullout specimens were casted and tested in this study. Three identical specimens for each group were prepared. The details of the testing matrix adopted in this study are shown in Table 2. The labeling system in this study was chosen so that it is easy to identify: volume fraction of fibers, concrete type, exposure duration, conditioning temperature, and the number of the specimen. For example, 0.5% SF-60-35-3 indicates the third SFRC specimen at 0.5% fiber volume fraction, exposed for 60 days at 35 °C. The pullout specimens consisted of concrete prisms with dimensions of 200 × 200 × 200 mm with the BFRP bars embedded in the center of the prism according to the ASTM D7913 [26]. Polypropylene tubes were used as bond breakers to break the bond between the BFRP bars and concrete to reduce the bottom plate's restraining effect [20]. The embedment length was chosen to be five times the diameter of the bar equivalent to 50 mm according to ASTM D7913 [26]. The BFRP bars were inserted in steel tubes filled with cementitious grout to prevent the breakage of the BFRP bars by the machine jaws, according to ASTM D7205 [27]. All specimens were casted horizontally in plywood formwork, as depicted in Fig. 2(a). The BFRP bars were protruded for 50 mm outside the concrete surface to measure the free end slippage. All specimens were cured for 28 days before the start of the conditioning by direct immersion in tap water. The control (unconditioned) specimens were stored for 90 days in a temperature-controlled room after curing.

Furthermore, sixty-three compressive strength cylinders were casted to track the compressive strength of the specimens throughout the environmental conditioning. In general, the compressive strengths tend to increase with exposure duration. Fig. 2(b) shows some of the pullout specimens and concrete cylinders after casting.

2.3. Environmental conditioning

Two galvanized steel tanks were fabricated and equipped with circulation pumps and heaters to simulate the environmental conditioning. The seawater was prepared artificially by adding NaCl in 3.9% concentration by weight and thoroughly mixing it before the placement of the specimens. The tanks were insulated with Rockwool sheets to prevent heat loss. Moreover, polyfoam was used to fill all existed openings to prevent excessive evaporation during the conditioning.

2.4. Test setup

All the tests were conducted using a universal testing machine (UTM) with a capacity of 1500 kN. As illustrated in Fig. 3, the steel frame setup had to be fabricated to test the pullout specimens. Two linear variable displacements transducers (LVDTs), with a capacity of 25 mm, were used to measure the free and loaded end slippages. The LVDTs were connected to the acquisition data logger capable of measuring one reading per second. The pullout test was done by applying a direct tensile load with a displacement control at a rate of 1.2 mm per min, according to ASTM D7913 [26].

3. Test results and discussion

The bond performance and durability results are shown in Table 2. The distribution of the bond stress is not uniform. Hence, the average bond stress is approximated using the following equation:

$$\tau = \frac{P}{\pi d_b L_d} \tag{1}$$

where τ is the bond stress along the embedment length, P is the maximum pullout force, d_b is the bar's diameter and L_d is the embedment length. The free end slippage was taken directly from the top LVDT readings, whereas the loaded end slippage was obtained by subtracting the bar's elongation at each reading from the bottom LVDT using the following equation:

$$\delta_{LE} = \text{Bottom LVDT reading} - \frac{PL}{AE} \tag{2}$$

where δ_{LE} is the loaded end slippage, P is the pullout force corresponding to the LVDT reading, L is the distance from the steel bracket to the beginning of the embedment length equivalent to 210 mm, A is the bar's cross-sectional area, and E is the modulus of elasticity of the bar.

3.1. Bond failure mechanism

All unconditioned specimens failed under pullout failure. The pullout failure was identified by exhibiting slippage during the reduction in the bond stress after reaching the peak stress. No cracks appeared on the concrete cube's surface that indicated a splitting failure. It was noticed that the interlaminar shear between the basalt fibers and the surrounding resin governed the mode of failure rather than concrete shearing. This was identified by splitting the pullout cubes and visually inspecting the bar's condition and the concrete's surface that is in direct contact with the bar. The crushed resin was noticed on the concrete surface along the embedment length. The concrete surface along the embedment length was intact and helically shaped with no signs of concrete shearing. A similar failure mode was reported by Achillidis and Pilakoutas [13] where the interlaminar shear between the fibers and the surrounding matrix being the governing factor for the mode of failure when the concrete compressive strength is higher than 30 MPa.

On the other hand, for plain concrete specimens exposed for 90 days at 60 °C, PC-90–60-3 had a rebar fracturing type of failure before reaching the peak load, and PC-90-60-1 exhibited a pullout mode of failure followed by rebar fracture. On the other hand, all conditioned SFRC specimens showed a typical pullout failure. These results indicate the predominance of the conditioning temperature and exposure duration on changing the failure type rather than the addition of steel fibers to concrete.

3.2. Bond-slip behavior

Representative bond-slip curves of the unconditioned and conditioned pullout specimens are shown in Figs. 4–6. All specimens showed an ascending branch up to a point where the maximum pullout stress is reached. This is attributed to the chemical adhesion and mechanical interlock of the BFRP bars to concrete, followed by a gradual reduction due to the wedging action of the bar's surface treatment. As depicted in Fig. 4, most of the maximum developed bond stress is attributed to the mechanical interlock rather than the chemical adhesion because the BFRP bars began to slip at a relatively low applied pullout load. This agrees well with the results reported by Achillides and Pilakoutas [13].

In terms of bond performance, the addition of steel fibers resulted in an improvement in the bond strength of 19.5% and 1.5% for 0.5% and 1% steel fiber volume fraction compared to plain concrete specimens. This improvement resulted from the fiber bridging effect after the initiation of cracks surrounding the BFRP bar due to the induced tensile stresses during the pullout test. Moreover, steel fibers exhibited adequate confining pressure that provided additional resistance to the pullout loads, which improved the bond strength. On the other hand, there was inconsistency in the bond strength improvement ratio, which implied that increasing V_f of steel fibers had an uncertain impact on the bond strength of BFRP bars. Similar observations were reported by Kim et al. [28]. It should be noted that the bond strength of the unconditioned specimens met the ACI 440.6M [29] minimum requirements (>9.6 MPa).

Furthermore, Fig. 7 shows the average free end slippage of the bars considering the conditioning temperature after 90 days of seawater

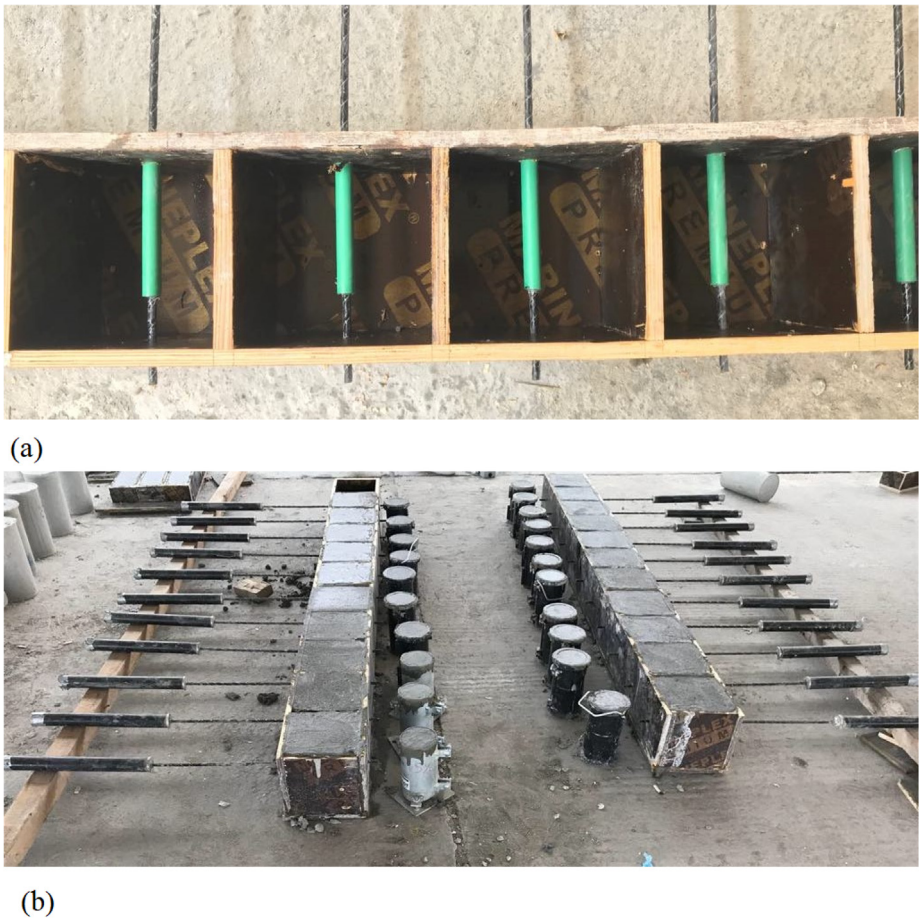

Fig. 2. (a) Plywood Molds; (b) Casted Specimens.

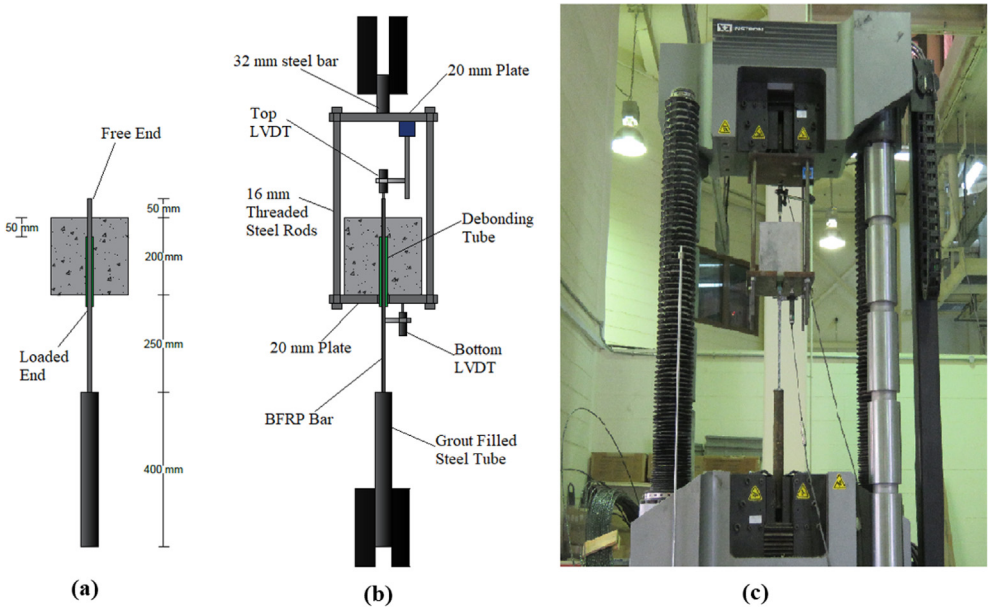

Fig. 3. (a) Specimens Dimensions; (b) Test Setup Layout; (c) Test Setup.

immersion. It can be observed that at a temperature of 60 °C, all specimens showed a decrease in slippage after 90 days of exposure compared to their control specimens and their counterpart specimens conditioned at 35 °C. This indicated that the reduction of slippage was mainly caused by the increase in conditioning temperature. This can be attributed to the reduced bond-slip initial toughness caused

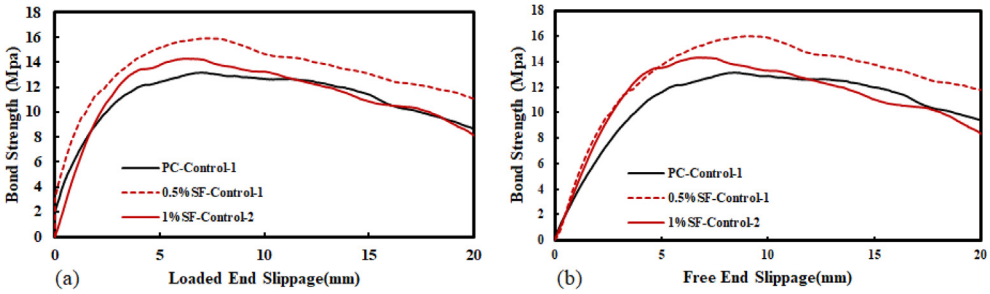

Fig. 4. Bond-Slip Cuves for Control Specimens: (a) Loaded End; (b) Free End Slippage.

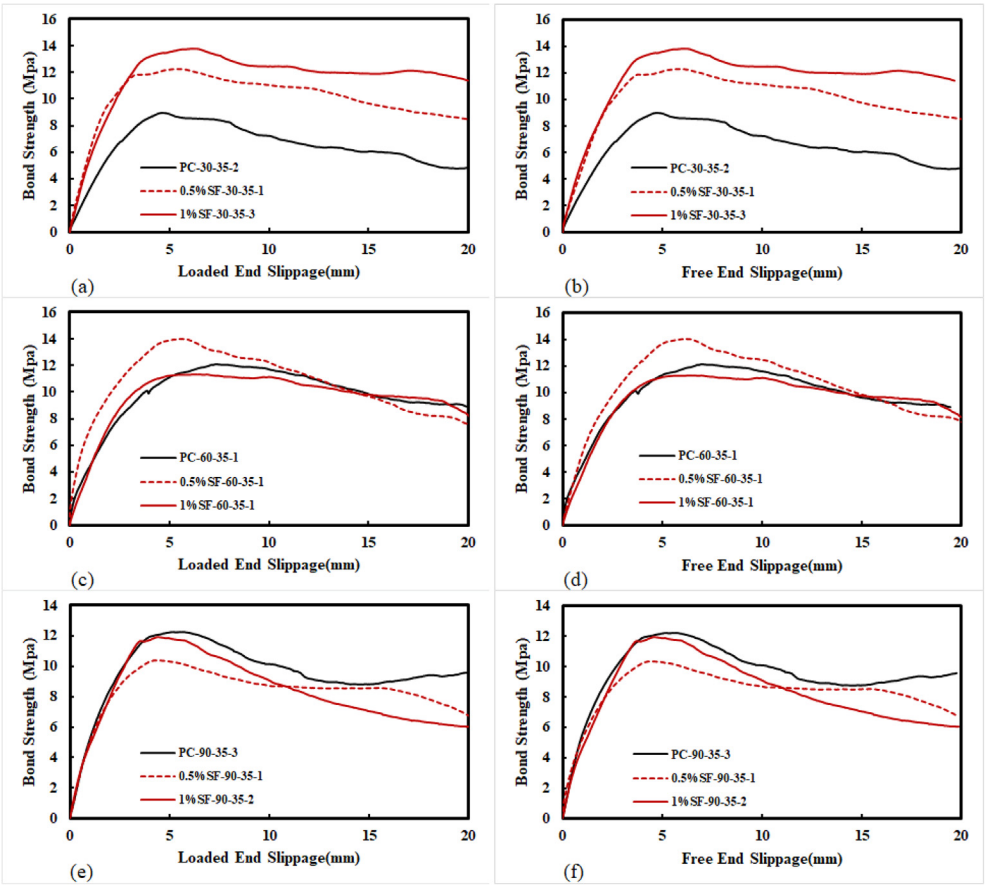

Fig. 5. Bond-Slip Curves for 35 °C Conditioned Specimens at Loaded and Free Ends: (a) 30 Days; (b) 30 Days; (c) 60 Days; (d) 60 Days; (e) 90 Days; (f) 90 Days.

by the increase in conditioning temperature, which in turn allowed the BFRP to reach the ultimate bond stress at relatively lower slippage for the same concrete type.

3.3. Bond degradation

3.3.1. Plain concrete specimens

Figs. 8–10 show the column charts representing the average bond strengths, bond strength retentions, and normalized bond strength (by taking off the effect of the compressive strength) considering the immersion temperature, concrete type, and exposure durations investigated in this study. The BFRP bars embedded in plain concrete showed reductions of 8% and 10% compared to their unconditioned specimens. One of the main reasons that has a detrimental influence on the bond strength is that the interlaminar shear between the fibers and surrounding polymeric resin can be severely affected with the presence of a saline environment [30,31]. Additionally, the high variation in the coefficient of thermal expansion (CTE) of the BFRP bars (22×10^{-6}/K) and that of concrete (14.5×10^{-6}/K) results in high differences in the rates of expansions and contractions between the FRP bars and concrete depending on the surrounding temperature of the seawater [23,32]. This allows the BFRP to apply radial bursting stresses on the surrounding concrete. When these applied stresses are higher than the concrete's tensile strength, cracks in the surrounding concrete develop, creating voids along the bonding length. The developed voids diminish the contact between the surrounding concrete and the BFRP bar and allow chloride ions and water molecules to fill these voids. These water molecules and chloride ions tend to dif-

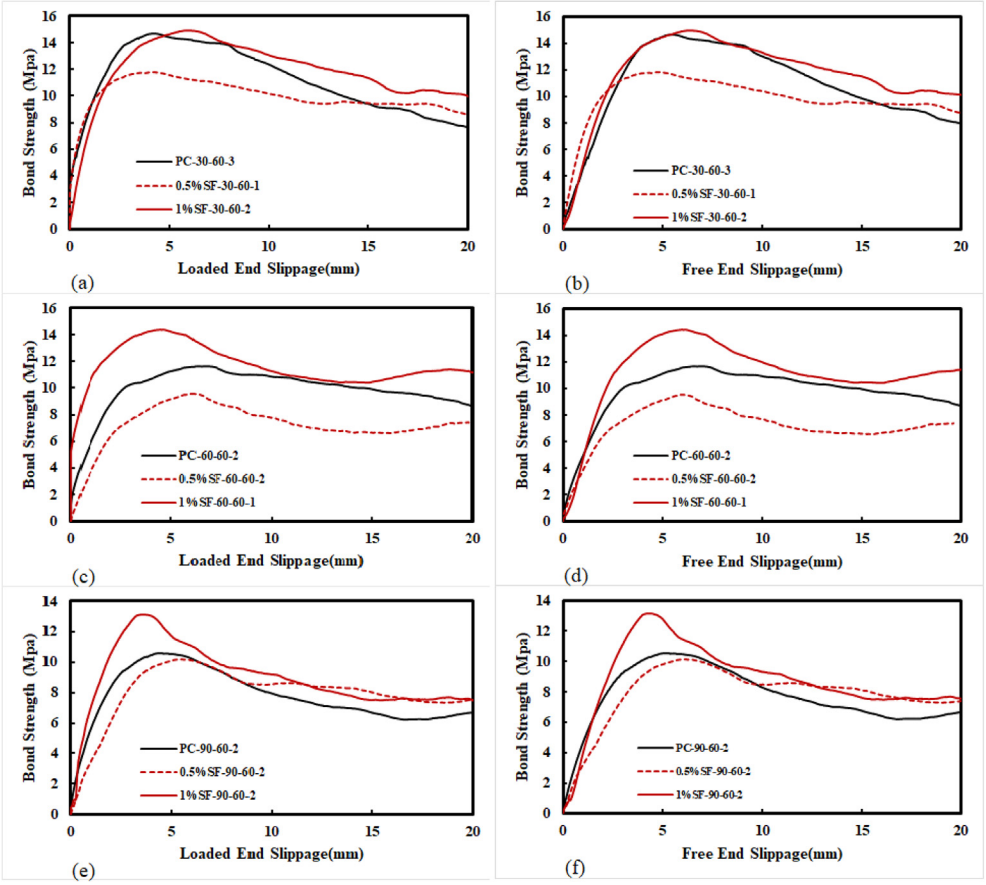

Fig. 6. Bond-Slip Curves for 60 °C Conditioned Specimens at Loaded and Free Ends: (a)& (B) 30 Days; (b) & (c) 60 Days; (e) & (f) 90 Days.

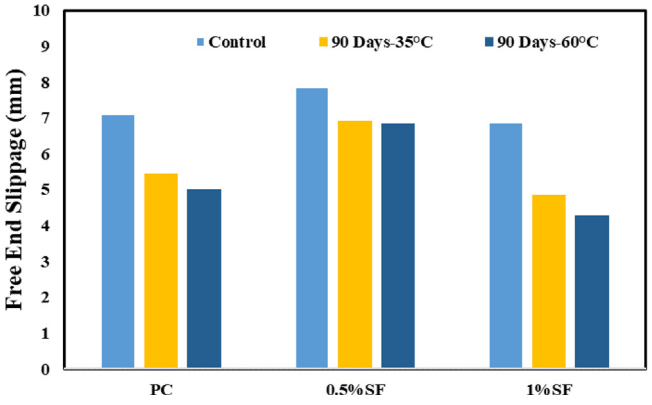

Fig. 7. Average Free End Slippage for Control and 90 days Conditioned Specimens.

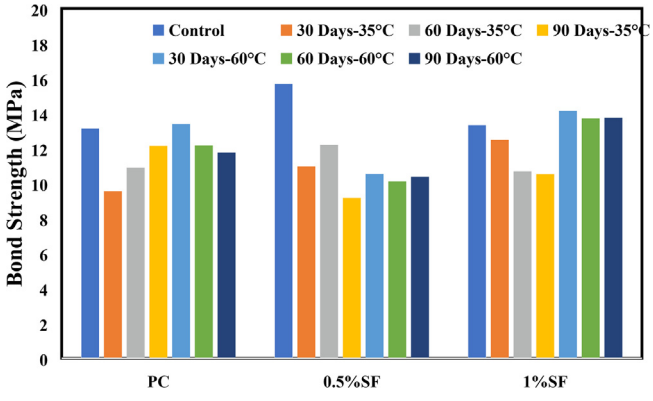

Fig. 8. Bond Strength with Exposure Time at Different Temperatures.

fuse into the polymeric resin, reducing the BFRP bar constituents' interlaminar shear and causing a higher rate of bond degradation. Consequently, increasing the immersion temperature surrounding the FRP bars accelerates the rate of moisture absorption [33] and chloride diffusion in concrete [34]. These reasons explain the higher reduction in the bond strength of plain concrete specimens when subjected to 60 °C immersion temperature compared to specimens subjected to 35 °C immersion temperature after 90 days of exposure.

On the contrary, it is worth noting that at 30 days of exposure at 60 °C immersion temperature, the bond strength increased to a point higher than that of the unconditioned specimens, followed by a decreasing trend in the bond strength with exposure time. This increase could be attributed to the bar swelling effect due to high moisture uptake by the polymeric resin, accelerated by the high temperature, which increases the interlock of the BFRP bar with the surrounding concrete [19,35]. Whereas for plain concrete specimens immersed at 35 °C, the bond strength tended to increase with exposure duration after 30 days of exposure, however this increase was not sufficient to retrace the bond strength of the control specimens indicating the severity of seawater conditioning. This may be explained by the slower rates of moisture absorption causing slower rates of bar swelling and the increase in the compressive strength, which counteracted the effect of seawater environment after 30 days of exposure compared to specimens exposed to 60 °C immersion temperature. Nevertheless, plain concrete specimens met the ACI 440.6M [29] minimum require-

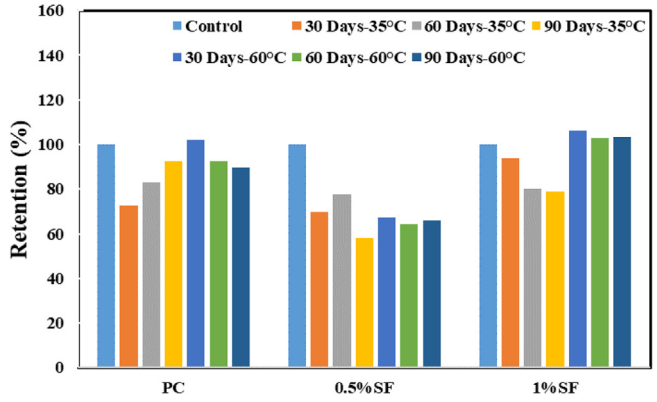

Fig. 9. Bond Strength Retentions with Exposure Time at Different Temperatures.

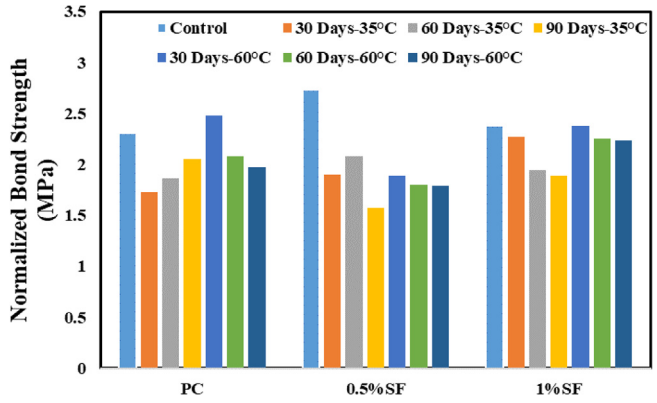

Fig. 10. Normalized Bond Strength with Exposure Time at Different Temperatures.

ments at the end of the environmental conditioning regardless of the immersion temperature.

3.3.2. SFRC specimens

As could be noticed from the pullout test results, the effect of high temperature tended to increase the bond strength of the BFRP bars with SFRC. Moreover, the increase in the steel fiber content significantly enhanced the bond strength of the conditioned specimens. This contradicts with the observation on the unconditioned specimens regarding the effect of fiber volume fraction on the bond performance. That being said, BFRP bars embedded in 0.5% SFRC exhibited significant bond strength reductions of 42% and 34% at 35 °C and 60 °C, respectively, compared to their (unconditioned) control specimens, revealing the unsuitability of using BFRP bars embedded in SFRC with low content of steel fibers in marine structures [36]. In contrast, the performance of SFRC with V_f = 1% resulted in a significant enhancement in the bond durability compared to SFRC with V_f = 0.5%. The BFRP bars embedded in SFRC with V_f = 1% exhibited a reduction of 21% at 35 °C and an improvement of 3% at 60 °C compared to the control specimens. Possible reasons for the obtained results are as follows: (1) the permeability and chloride diffusivity tend to significantly increase with the addition of steel fibers when compared to plain concrete due to the high conductivity of steel fibers [37], allowing more water molecules and chloride ions to diffuse in the polymeric resin at lower temperatures, hence accelerating the bond degradation rate when compared to plain concrete; (2) the high temperature tends to accelerate the corrosion of steel fibers [38], and due to the early stages of corrosion, the compressive strength of SFRC and bonding

Fig. 11. Corrosion of Steel Fibers in SFRC.

of steel fibers with surrounding concrete increase significantly [36,39–41], which in turn improves bond strength of BFRP bar with concrete due to the additional confinement and more effective crack bridging; (3) with increased time of immersion in aqueous solution, the increase in the content of steel fibers tend to significantly decrease the permeability of concrete due to the reduction of concrete shrinkage and the continuity destruction of porous channels by the fiber mechanism [42], limiting the access of water molecules and chloride ions to diffuse further in the polymeric resin. That being said, corrosion pits at the concrete surface were observed for SFRC after 30 days of immersion at 60 °C indicating the early initiation of corrosion and more being obvious at the high content of steel fibers, as shown in Fig. 11. This signals the destruction of the oxide layer surrounding the steel fibers due to concrete carbonation which led to: (1) significant improvement in compressive strength; (2) less chloride ions diffusion;(3) less water molecules uptake by the resin; and (4) high bond between the steel fiber-concrete interface leading to the significant improvement in the bond strength compared to specimens exposed at a lower temperature of 35 °C. The BFRP bars embedded in SFRC at 60 °C experienced no reduction in the bond strength after 60 days of exposure regardless of the steel fibers volume fraction. Whereas at 35 °C, the different volume fractions exhibited different trends with a clear decreasing trend for 1% steel fiber with a slight reduction after 60 days of exposure, unlike 0.5% steel fiber which caused the bond of the BFRP bars to increase until 60 days followed by a significant reduction afterward. This could be attributed to the rate of chloride diffusion and the effect of increasing the fiber content with long periods of immersion on decreasing or limiting the concrete permeability. The minimum bond strength of BFRP bars embedded in 0.5% SFRC after 90 days of exposure was found to be 9.16 MPa at 35 °C which did not meet the requirement of the ACI 440.6M [29] (>9.6 MPa),

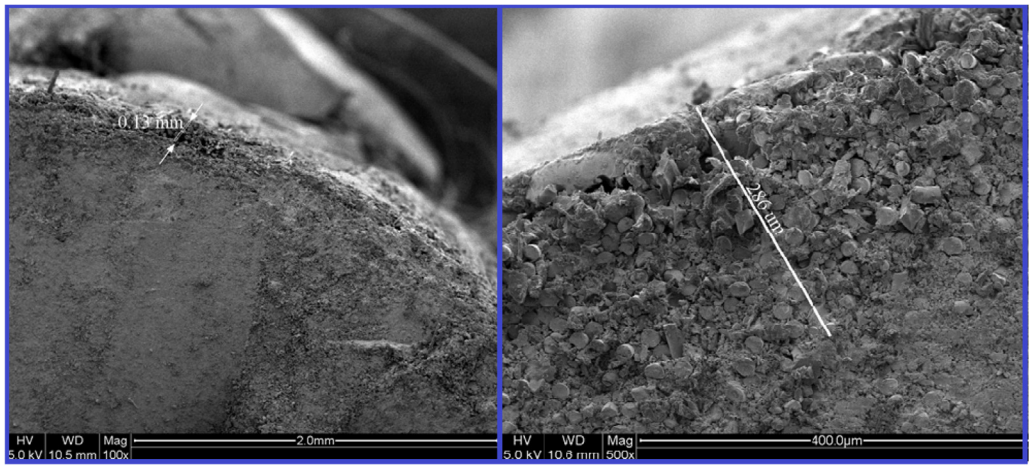

(a) 100x 500x

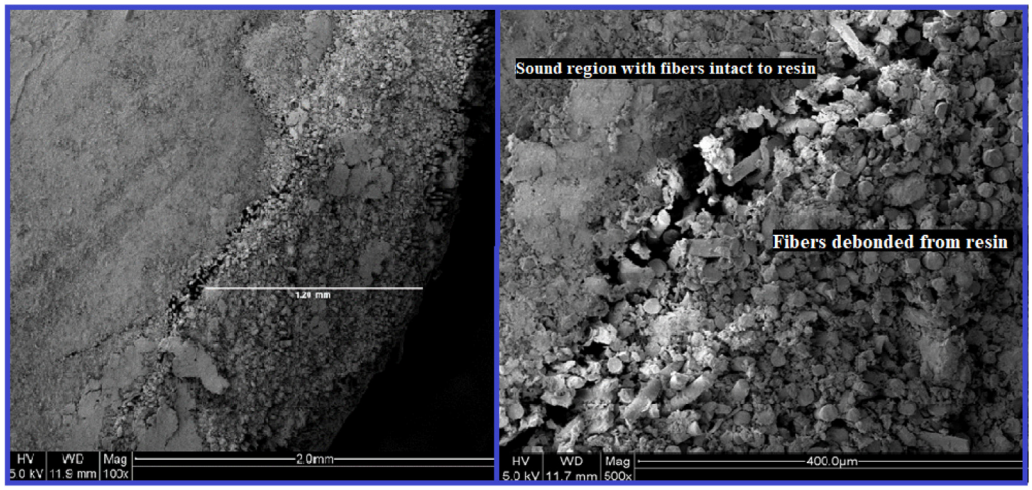

(b) 100x 500x

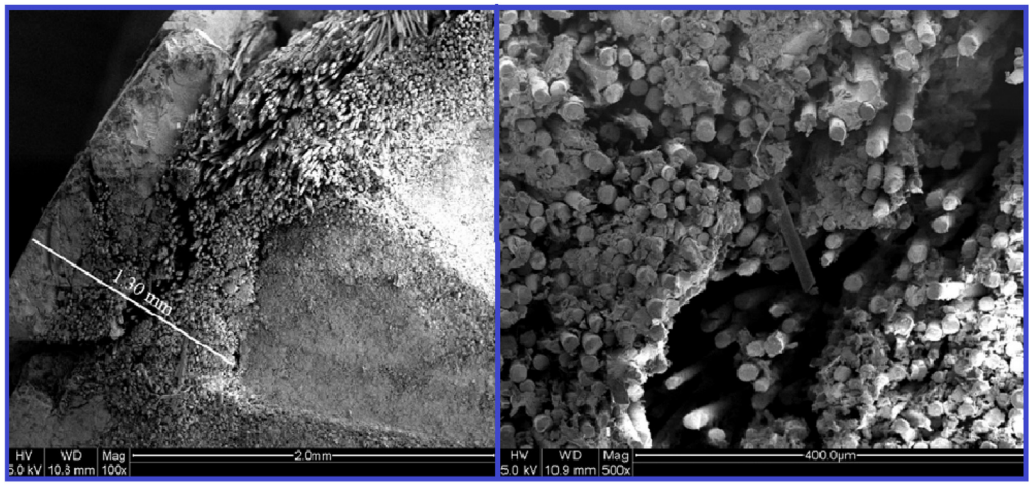

(c) 100x 500x

Fig. 12. SEM Images plain concrete: (a) Control; (b) 90 Days – 35 ˚C; (c) 90 Days-60 ˚C.

Table 3
BPE and CMR Proposed Values.

Specimen	BPE α	CMR Sr	β	S_m (mm)	τ_m (MPa)
Unconditioned (Control) Specimens					
PC-Control	0.4254	2.218	0.9563	7.1	13.14
0.5%SF-Control	0.486	2.0154	1.1982	7.85	15.7
1%SF-Control	0.4802	1.6042	1.5012	6.87	13.34
30 Days Conditioned Specimens at 35 °C					
PC-30–35	0.5345	1.5824	1.4382	6.17	9.547
0.5%SF-30–35	0.4653	1.4578	1.2512	5.6	10.97
1%SF-30–35	0.4493	1.4866	1.5393	6.92	12.49
30 Days Conditioned Specimens at 60 °C					
PC-30–60	0.4933	1.5991	1.4536	6.37	13.4
0.5%SF-30–60	0.4996	1.4073	1.3176	5.24	10.54
1%SF-30–60	0.4753	1.4133	1.5789	6.31	14.15
60 Days Conditioned Specimens at 35 °C					
PC-60–35	0.4481	1.6977	0.9702	5.56	10.9
0.5%SF-60–35	0.4342	1.8365	1.2565	7.69	12.21
1%SF-60–35	0.4002	1.5664	1.3017	7.34	10.69
60 Days Conditioned Specimens at 60 °C					
PC-60–60	0.4834	1.4548	1.3355	5.51	12.17
0.5%SF-60–60	0.4361	1.6341	1.0395	5.83	10.12
1%SF-60–60	0.5407	1.254	1.6434	5.14	13.72
90 Days Conditioned Specimens at 35 °C					
PC-90–35	0.5219	1.346	1.6498	5.44	12.14
0.5%SF-90–35	0.4264	1.9568	1.0697	6.92	9.157
1%SF-90–35	0.5755	1.3115	1.7301	4.84	10.53
60 Days Conditioned Specimens at 60 °C					
PC-90–60	0.4272	1.8311	0.9619	6.23	11.77
0.5%SF-90–60	0.5342	1.8672	1.4496	6.84	10.37
1%SF-90–60	0.5259	1.7398	1.3143	4.29	13.76

Note: S_m: Bar slippage corresponding to maximum bond stress; τ_m: Maximum bond stress

revealing the unsuitability of using the adopted bars in SFRC with steel fiber volume fraction of 0.5% in marine structures if the ACI specifications are to be adopted.

3.4. Scanning electron microscopy (SEM) analysis

The cross-sections of the BFRP bars embedded in plain concrete of the control specimens and specimens conditioned for 90 days at 35 °C and 60 °C were inspected using SEM analysis. After splitting the concrete, the BFRP bars' samples were extracted from locations that are in direct contact with concrete. The SEM analysis aimed at investigating the interfacial bond between the BFRP bar's fibers and polymeric resin by observing the defected region due to environmental conditioning. Fig. 12 shows the SEM images at different magnifications for the BFRP bars' cross-sections investigated in this study. The SEM images confirmed the observed results at pullout tests that immersion of plain concrete pullout specimens in seawater had a detrimental impact on the interfacial bond between the fibers and the polymeric resin. As could be noticed in Fig. 12(b) and (c), the defected regions of the conditioned specimens were more prominent than that of the unconditioned specimens as depicted in Fig. 12(a). Moreover, as shown in Fig. 12(c), BFRP specimens conditioned at 60 °C show a larger defected area, from the outer surface of the bar towards the center, than that of the specimens conditioned at 35 °C. This confirms the effect of increasing the immersion temperature in accelerating the ingress of aggressive solution in the BFRP bars, which in turn weakened the interfacial bond between the polymeric resin and the basalt fibers.

4. Theoretical analysis

The BPE model, proposed by Eligehausen et al.[43], describes the bond-slip behavior of steel reinforcement with concrete. However, this model was found to be reliable in describing the ascending branch of the bond-slip behavior of FRP reinforcements [1,22]. The following equation describes the ascending branch by the BPE model:

$$\frac{\tau}{\tau_b} = \left(\frac{s}{s_b}\right)^{\alpha} \quad for \quad 0 \le s \le s_b \tag{3}$$

where τ_b and s_b are the maximum pullout stress and its corresponding slippage, respectively. α is a curve-fitting parameter that should be less than 1 to be meaningful physically and is obtained using the least square residuals method.

Furthermore, the CMR model was proposed by Consenza et al. [44] to describe the ascending branch of the bond-slip curve of FRP bars more effectively. The ascending branch by the CMR model can be expressed in the following equation:

$$\frac{\tau}{\tau_b} = \left(1 - \exp\left(-\frac{s}{s_r}\right)\right)^{\beta} \tag{4}$$

where τ_b is the ultimate bond stress. S_r and β are curve-fitting parameters.

All the 63 pullout specimens were modeled using the BPE and CMR models to calibrate the values taking into account the conditioning temperature, duration of exposure, and fiber volume fractions adopted in this study. Since almost all structural problems consider the serviceability limit states, only the ascending branches of the bond slip curves have been modeled. The average values for the parameters of these models are listed in Table 3. For the BPE model, the average proposed values of the curve fitting parameter, α, for unconditioned plain concrete, 0.5% SFRC, and 1% SFRC were 0.43, 0.41, and 0.46, respectively. Regarding the CMR model, for control specimens, the proposed values of S_r and β were 2.22 and 0.96 for plain concrete, 2.02 and 1.2 for 0.5%SFRC, and 1.6 and 1.5 for 1% SFRC. Fig. 13 shows representative modeling of the experimental data of

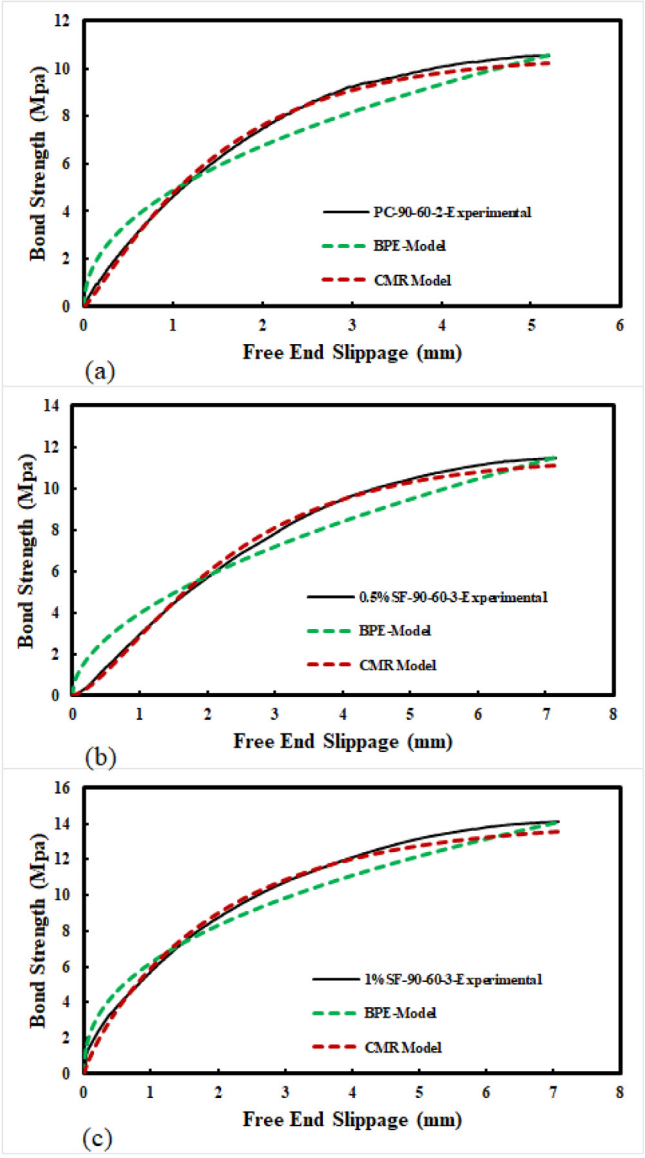

Fig. 13. Experimental Data Vs. BPE and CMR Models for Conditioned Specimens to Saline Solution after 90 Days at 60 oC of (a) Plain Concrete; (b) 0.5% SFRC; (c) 1% SFRC.

conditioned specimens for 90 days at 60 ˚C. The CMR model showed better correlation with the experimental data of this study due to its ability to have an infinite slope at the beginning of the ascending branch and the presence of the exponential term that allows it to have a better presentation for the ascending branch for the bond-slip curve of FRP bars.

5. Service life prediction

The service life predictions for the 50 years of service life bond strength retentions were performed based on the short-term durability test done on this study. The method mentioned in the fib Bulletin 40 [45] was adopted in the service life predictions for plain concrete specimens in addition to the modification mentioned by Serbescu et al. [46] for the case of SFRC specimens. The method by the fib Bulletin 40 [45] involves an environmental reduction factor, $\eta_{env,b}$, which is obtained using the following equations:

$$\eta_{env,b} = 1/[(100 - R_{10})/100]^n \quad (5)$$

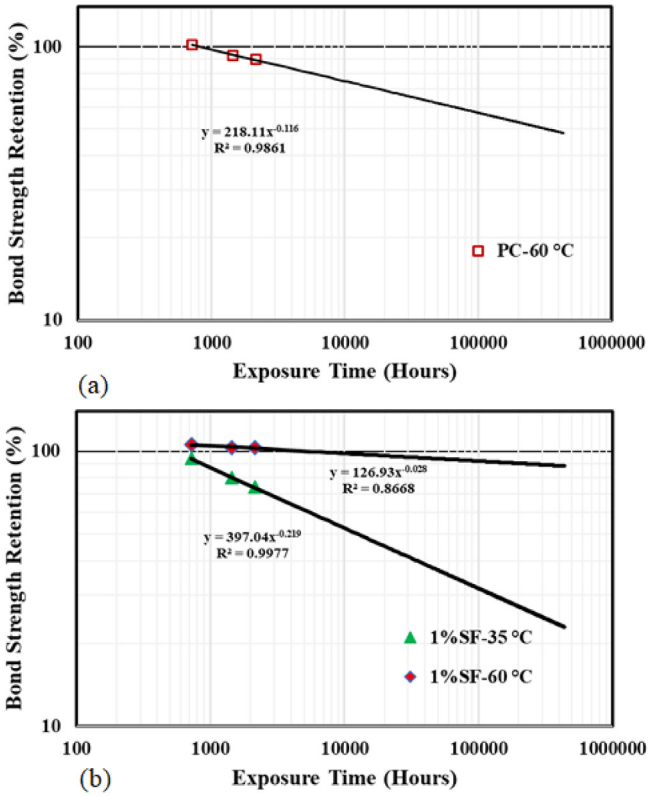

Fig. 14. Bond Strength Retention Curve of HWBFRP Bars Embedded in:(a) Plain Concrete; (b) 1% SFRC.

$$n = n_{mo} + n_T + n_{SL} \quad (6)$$

where the parameters n_{mo}, n_T, and n_{SL} are parameters that consider the humidity, temperature, and required service life respectively. The standard reduction factor in percent per decade, R_{10}, of the bond strength can be obtained from the slope of the degradation line when fitted in a double logarithmic scale. The points that make up the degradation line are the retention values obtained at the adopted exposure durations of the study. The R-square of the fitted line must be >0.8 for this method to be applicable. Therefore, this method was only valid for plain concrete specimens and 1% SFRC specimens. For plain concrete specimens, the degradation line at 60 ˚C was used because it showed degradation in the bond strength with exposure time, whereas for 1% SFRC both degradation lines, at 35 ˚C and 60 ˚C, were adopted since, at both immersion temperature, the bond strengths tended to decrease with exposure time. Therefore, the method proposed by Serbesco [97] can be applied to take into account both conditioning temperatures. The service life adopted in this study is 50 years which leads to a value of n_{SL} equals to 2.7 according to the fib Bulletin 40 [45], assuming moisture-saturated conditions. n_T equals to 1 at 35 ˚C according to the fib Bulletin 40 [45] and to 2.5 at 60 ˚C in accordance to Serbescu et al. [46]. Fig. 14(a) shows the degradation line of the plotted retentions for 30, 60, and 90 days at 60 ˚C of BFRP bars embedded in plain concrete. This leads to an R_{10} value of 11.6% for plain concrete specimens. After 50 years of service life, the predicted bond strength retention was 48%. Consequently, as shown in Fig. 14(b), for 1% SFRC specimens, the average slope of the two degradation lines can be adopted based on the modification method proposed by Serbescu et al. [46] to simulate their bond degradation. This yields an R_{10} value of 12.35% resulting in bond retentions of 80 and 26% at 35 and 60 ˚C after 50 years of service life. However, using the fib Bulletin 40 [42] method, the value of R10 is 2.8%, resulting in bond retention

Table 4
Service Life Prediction.

					Plain Concrete		Steel FRC	
n_{SL}	n_{mo}	MAT (°C)	n_T	n	$\eta_{env,b}$	$1/\eta_{env,b}$ (%)	$\eta_{env,b}$	$1/\eta_{env,b}$ (%)
2.7 (50 years of service life)	−1(Dry)	<5	−0.5	1.2	1.16	86	1.17	85
		(5–15)	0	1.7	1.23	81	1.25	80
		(15–25)	0.5	2.2	1.31	76	1.34	75
		(25–35)	1	2.7	1.4	72	1.43	70
	0(Moist)	<5	−0.5	2.2	1.31	76	1.34	75
		(5–15)	0	2.7	1.4	72	1.43	70
		(15–25)	0.5	3.2	1.48	67	1.52	66
		(25–35)	1	3.7	1.58	63	1.63	61
	1(MoistureSaturated)	<5	−0.5	3.2	1.48	67	1.52	66
		(5–15)	0	3.7	1.58	63	1.63	61
		(15–25)	0.5	4.2	1.68	60	1.74	57
		(25–35)	1	4.7	1.79	56	1.86	54

of 88% at 60 °C after 50 years of service life. These significant differences in the R_{10} values obtained by the two methods are attributed to the early stages of corrosion of the steel fibers, which resulted in an increase in the bond of the steel fibers with the surrounding concrete, a noticeable increase in the compressive strength, and a reduction in the diffusion rates of moisture and chloride ions (Cl^-) in the polymeric resin. These effects are not taken into consideration in Eq. (5).

Table 4 shows the retentions of the bond strength considering dry, moist, and moisture saturated exposure conditions resulted from Eq. (5). Depending on the mean annual temperatures (MATs) for the adopted service life of 50 years, the bond strength retention values ranged from 56% to 86% for BFRP bars embedded in plain concrete. On the other hand, the bond strength retentions of BFRP bars embedded in 1% SFRC showed a slight reduction in the bond durability that varied from 1% to 4% in cases of dry, moist, and moisture saturated conditions compared to plain concrete, indicating the unsuitability of using the BFRP bars embedded in SFRC in marine structures as long as the cost is concerned. Further investigations are needed to validate the proposed model taking into account different parameters.

6. Conclusions

This paper presented bond durability investigations of BFRP bars embedded in plain concrete and SFRC taking into account the effects of immersion temperature, exposure duration, and steel fibers volume fractions. Moreover, the durability assessment was done through failure types, bond-slip behavior, degradation of the bond, and SEM analysis. Furthermore, the BPE and CMR models were calibrated to take into account the parameters of this study, hence values of the models' parameters were proposed. Consequently, the service life prediction model according to the method in the fib Bulletin 40 [45] and the modification by Sebescu et al. [46] was proposed. The following conclusions can be drawn based on the obtained results of this study:

1. The bond strength of the unconditioned specimens improved with the addition of steel fibers to concrete. The enhancement was 19.5% when 0.5% SFRC was used, whereas a negligible improvement was noticed when 1% SFRC was used compared to plain concrete. These results indicate that increasing V_f of steel fiber has an uncertain impact on the bond strength of BFRP bars.
2. The types of failure observed in this study were typical pullout and rebar fracturing failures. The increase in the immersion temperature had the most significant effect on the type of failure among all parameters investigated in this study.
3. Increasing the immersion temperature led to a reduction in the free end slippage regardless of the fibers volume fraction when specimens at 90 days of exposure were compared to unconditioned specimens.
4. BFRP bars embedded in plain concrete showed higher reduction when the immersion temperature increased. Unlike SFRC specimens which seemed to be uninfluenced by the increase in immersion temperature but rather affected by the presence of the corrosive solution containing high concentrations of NaCl by short-term durability tests.
5. At 35 °C, SFRC specimens showed the highest degradation compared to their unconditioned counterpart SFRC specimens with a reduction of 42% and 21% for V_f = 0.5 and 1%, respectively. On the other hand, at 60 °C, SFRC specimens possessed a reduction of 34% in case of 0.5% SFRC and an improvement of 3% in case of 1% SFRC compared to their counterpart control specimens.
6. According to the SEM analysis of this study, increasing the immersion temperature in seawater accelerates the deterioration of interfacial bond between the basalt fibers and the polymeric resin
7. Based on the service life prediction model proposed in this paper, for plain concrete specimens, the least retentions were 72, 63, and 56% in dry, moist, and moisture saturated environmental conditions, respectively. On the other hand, the lowest bond strength retentions in the case of 1% SFRC were 70, 61, and 54% in dry, moist, and moisture saturated, indicating a slight reduction of 1 to 4% compared to plain concrete. This is attributed to the significant reduction exhibited by 1% SFRC subjected to 35 °C.

The obtained results of this paper are restricted to the parameters investigated. Therefore, future research is recommended to carry out the test for a longer duration to validate the prediction model presented. In addition, the results of this study revealed that the addition of steel fibers to normal strength concrete is not complementary to BFRP when utilized in marine structures. Even though the addition of high content of steel fibers resulted in an enhanced durability performance, this addition may not be cost-effective since a comparable or even better bond performance can be achieved with plain concrete. However, in actual applications of BFRP bars, the BFRP bars are subjected to tensile loads, which may cause higher degradation rates in which the effect of the steel fibers comes into action. Therefore, further investigations are required in this matter.

7. Data availability

Data availability The raw/processed data required to reproduce these findings cannot be shared at this time as the data also forms part of an ongoing study.

Declaration of Competing Interest

The authors declare that they have no known competing financial interests or personal relationships that could have appeared to influence the work reported in this paper.

Acknowledgments

The authors show their gratitude to Qatar University for their financial support through the internal grant no. QUST-1-CENG-2020-17. Also, this publication was made possible by GSRA grant no. GSRA7-1-0419-20019 from the Qatar National Research Fund (QNRF, a member of Qatar Foundation). The findings achieved herein are solely the responsibility of the authors. Open Access funding provided by the Qatar National Library.

References

[1] El Refai A, Ammar MA, Masmoudi R. Bond performance of basalt fiber-reinforced polymer bars to concrete. J Compos Constr 2015;19:1–12. https://doi.org/10.1061/(ASCE)CC.1943-5614.0000487.
[2] Attia K, Alnahhal W, Elrefai A, Rihan Y. Flexural behavior of basalt fiber-reinforced concrete slab strips reinforced with BFRP and GFRP bars. Compos Struct 2019;211:1–12. https://doi.org/10.1016/J.COMPSTRUCT.2018.12.016.
[3] Attia K, El Refai A, Alnahhal W. Flexural behavior of basalt fiber-reinforced concrete slab strips with BFRP bars: experimental testing and numerical simulation. J Compos Constr 2020;24:04020007. https://doi.org/10.1061/(ASCE)CC.1943-5614.0001002.
[4] Abushanab A, Alnahhal W. Performance of basalt fiber reinforced continuous beams with basalt FRP bars. IOP Conf Ser Mater Sci Eng 2020;910:. https://doi.org/10.1088/1757-899X/910/1/012004012004.
[5] Hassan M, Benmokrane B, Elsafty A, Fam A. Bond durability of basalt- fi ber-reinforced-polymer (BFRP) bars embedded in concrete in aggressive environments 2016;106:262–72.
[6] Jamshaid H, Mishra R. A green material from rock: basalt fiber – a review. J Text Inst 2016;107:923–37. https://doi.org/10.1080/00405000.2015.1071940.
[7] Davalos JF, Chen Y, Ray I. Effect of FRP bar degradation on interface bond with high strength concrete. Cem Concr Compos 2008;30:722–30. https://doi.org/10.1016/j.cemconcomp.2008.05.006.
[8] Robert M, Benmokrane B. Effect of aging on bond of GFRP bars embedded in concrete. Cem Concr Compos 2010;32:461–7. https://doi.org/10.1016/J.CEMCONCOMP.2010.02.010.
[9] Ametrano D. Bond characteristics of glass fibre reinforced polymer bars embedded in high performance and ultra-high performance concrete 2011.
[10] Shen D, Ojha B, Shi X, Zhang H, Shen J. Bond stress – slip relationship between basalt fiber-reinforced polymer bars and concrete using a pull-out test 2016. DOI:10.1177/0731684415627504.
[11] Hossain KMA, Sennah K. Bond Strength of Ribbed GFRP Bars Embedded in High Performance Fiber Reinforced Concrete 2015;2:1260–7.
[12] Universit M. Evaluation of Bond Strength of FRP Reinforcing Rods in Concrete and FE Modelling Evaluation of Bond Strength of FRP Reinforcing Rods in Concrete and 2017.
[13] Achillides Z, Pilakoutas K. Bond behavior of fiber reinforced polymer bars under direct pullout conditions. J Compos Constr 2004;8:173–81. https://doi.org/10.1061/(ASCE)1090-0268(2004)8:2(173).
[14] Erdem S, Kağnıcı T, Blankson MA. Investigation of Bond between Fibre Reinforced Polymer (FRP) Composites Rebar and Aramid Fibre-Reinforced Concrete 2015;5:148–54. DOI:10.5923/j.cmaterials.20150506.02.
[15] Ding Y, Ning X, Zhang Y, Pacheco-torgal F, Aguiar JB. Fibres for enhancing of the bond capacity between GFRP rebar and concrete 2014;51:303–12.
[16] Bi Q, Wang H. Bond strength of BFRP bars to basalt fiber reinforced high-strength concrete. In: Adv. FRP Compos. Civ. Eng. - Proc. 5th Int. Conf. FRP Compos. Civ. Eng. CICE 2010. p. 576–80. https://doi.org/10.1007/978-3-642-17487-2_125.
[17] Sólyom S, Balázs GL. Influence of FRC on bond characteristics of FRP reinforcement. In: Proc. 11th fib Int PhD Symp. Civ. Eng. FIB 2016. p. 271–8.
[18] Belarbi A, Wang H. Bond-Slip Response of FRP Reinforcing Bars in Fiber Reinforced Concrete under Direct Pullout n.d.:1–10.
[19] El Refai A, Abed F, Altalmas A. Bond durability of basalt fiber-reinforced polymer bars embedded in concrete under direct pullout conditions. J Compos Constr 2015;19:1–11. https://doi.org/10.1061/(ASCE)CC.1943-5614.0000544.
[20] Dong Z, Wu G, Xu B, Wang X, Taerwe L. Bond durability of BFRP bars embedded in concrete under seawater conditions and the long-term bond strength prediction 2016;92:552–62.
[21] Dong Z, Wu G, Zhao X, Asce F, Lian J. Long-Term Bond Durability of Fiber-Reinforced Polymer Bars Embedded in Long-Term Bond Durability of Fiber-Reinforced Polymer Bars Embedded in Seawater Sea-Sand Concrete under Ocean Environments 2018. DOI:10.1061/(ASCE)CC.1943-5614.0000876.
[22] Yan F, Lin Z. Bond durability assessment and long-term degradation prediction for GFRP bars to fiber-reinforced concrete under saline solutions. Compos Struct 2017;161:393–406. https://doi.org/10.1016/j.compstruct.2016.11.055.
[23] Belarbi A, Wang H. Bond durability of FRP bars embedded in fiber-reinforced concrete. J Compos Constr 2012;16:371–80. https://doi.org/10.1061/(ASCE)CC.1943-5614.0000270.
[24] Taha A, Alnahhal W, Alnuaimi N. Bond durability of basalt FRP bars to fiber reinforced concrete in a saline environment. Compos Struct 2020;243:. https://doi.org/10.1016/j.compstruct.2020.112277112277.
[25] I. Gutnikov S, S. Zhukovskaya E, S. Popov S, I. Lazoryak B. Correlation of the chemical composition, structure and mechanical properties of basalt continuous fibers. AIMS Mater Sci 2019;6:806–32. DOI:10.3934/matersci.2019.5.806.
[26] D7913/D7913M-14. Standard test method for bond strength of fiber-reinforced polymer matrix composite bars to concrete by pullout testing. ASTM Stand 2014:1–9. 10.1520/D7913.
[27] Carbon- P, Rod GP, Materials C, Precision S, Axial C, Application F. Standard Test Method for Tensile Properties of Fiber Reinforced Polymer Matrix 2018;i:1–13. 10.1520/D7205.
[28] Kim B, Doh J-H, Yi C-K, Lee J-Y. Effects of structural fibers on bonding mechanism changes in interface between GFRP bar and concrete. Compos Part B Eng 2013;45:768–79. https://doi.org/10.1016/j.compositesb.2012.09.039.
[29] ACI Committee 440.6-08(17). Specification for carbon and glass fiber-reinforced polymer bar materials for concrete reinforcement (Reapproved 2017). American Concrete Institute; 2017.
[30] Tam L ho, He L, Wu C. Molecular dynamics study on the effect of salt environment on interfacial structure, stress, and adhesion of carbon fiber/epoxy interface. Compos Interfaces 2019;26:431–47. DOI:10.1080/09276440.2018.1506901.
[31] Liu Q, Shaw MT, Parnas RS, Shaw MT, Parnas RS, McDonnell AM. Investigation of basalt fiber composite aging behavior for applications in transportation. Polym Compos 2006;27:475–83. https://doi.org/10.1002/pc.20215.
[32] Ceroni F, Cosenza E, Gaetano M, Pecce M. Durability issues of FRP rebars in reinforced concrete members. Cem Concr Compos 2006;28:857–68. https://doi.org/10.1016/j.cemconcomp.2006.07.004.
[33] Grammatikos SA, Zafari B, Evernden MC, Mottram JT, Mitchels JM. Moisture uptake characteristics of a pultruded fibre reinforced polymer flat sheet subjected to hot/wet aging. Polym Degrad Stab 2015;121:407–19. https://doi.org/10.1016/j.polymdegradstab.2015.10.001.
[34] Touil B, Ghomari F, Bezzar A, Khelidj A, Bonnet S. Effect of Temperature on Chloride Diffusion in Saturated Concrete. ACI Mater J 2017;114:713–21. DOI:10.14359/51688929.
[35] Saadatmanesh H (Hamid), Ehsani MR (Mohammad R, University of Arizona. Department of Civil Engineering. S, Rosas J. Fiber composites in infrastructure: proceedings of the Second International Conference on Composites in Infrastructure, ICCI'98, Tucson, Arizona, USA, 5-7 January, 1998. vol. 2. Department of Civil Engineering and Engineering Mechanics, University of Arizona; 1998.
[36] Frazão C, Camões A, Barros J, Gonçalves D. Durability of steel fiber reinforced self-compacting concrete. Constr Build Mater 2015;80:155–66. https://doi.org/10.1016/j.conbuildmat.2015.01.061.
[37] Afroughsabet V, Biolzi L, Monteiro PJM. The effect of steel and polypropylene fibers on the chloride diffusivity and drying shrinkage of high-strength concrete. Compos Part B Eng 2018;139:84–96. https://doi.org/10.1016/j.compositesb.2017.11.047.
[38] Prawoto Y, Ibrahim K, Nik WBW. Effect of ph and chloride concentration on the corrosion of duplex stainless steel. Arab J Sci Eng 2009;34:115–27.
[39] Alizade E, Jandaghi Alaee F, Zabihi S. Effect of steel fiber corrosion on mechanical properties of steel fiber reinforced concrete. Asian J Civ Eng 2016;17:147–58.
[40] Alwan JM, Naaman AE, Hansen W. Pull-out work of steel fibers from cementitious composites: analytical investigation. Cem Concr Compos 1991;13:247–55. https://doi.org/10.1016/0958-9465(91)90030-L.
[41] Frazão C, Barros J, Camões A, Alves AC, Rocha L. Corrosion effects on pullout behavior of hooked steel fibers in self-compacting concrete. Cem Concr Res 2016;79:112–22. https://doi.org/10.1016/j.cemconres.2015.09.005.
[42] Singh AP, Singhal D. Permeability of steel fibre reinforced concrete influence of fibre parameters. Procedia Eng 2011;14:2823–9. https://doi.org/10.1016/j.proeng.2011.07.355.
[43] Eligehausen R, Popov EP, Bertero V. Local bond stress-slip relationships of deformed bars under generalized excitations, University of California, report no UCB/EERC-83/23 of the National Science Foundation. In Proc 7th Eur Conf Earthq Eng 1983:69–80. Report No. UCB/EERC-83/23.
[44] Cosenza E, Manfredi G, Realfonzo R. Analytical modelling of bond between FRP reinforcing bars and concrete. Non-Metalic Reinf Concr Struct Reinf Concr Struct 1995:164–71. https://doi.org/10.1145/2505515.2507827.
[45] fib TG 9.3. fib Bulletin 40: FRP reinforcement in RC structures. fib. The International Federation for Structural Concrete; 2002. DOI:10.35789/fib.BULL.0040.
[46] Serbescu A, Guadagnini M, Pilakoutas K. Mechanical characterization of basalt FRP rebars and long-term strength predictive model. J Compos Constr 2015;19:04014037. https://doi.org/10.1061/(ASCE)CC.1943-5614.0000497.